Detecting the time-dependent coherence between non-stationary electrophysiological signals –A combined statistical and time-frequency approach

Yang Zhan[†] David Halliday[†] Xuguang Liu[*] Jianfeng Feng[‡]

[†]Department of Electronics, University of York

York, YO10 5DD, UK

[*] Charing Cross Hospital & Division of Neuroscience and Mental Health

Imperial College London, London, W6 8RF, UK

[‡]Department of Computer Science and Mathematics

University of Warwick, Coventry, CV4 7AL, UK

Research Article

December 6, 2005

Abstract

Various time-frequency methods have been used to study the time-varying properties of non-stationary neurophysiological signals. In the present study, a time-frequency coherence using continuous wavelet transform (CWT) together with its confidence intervals are proposed to evaluate the correlation between two non-stationary processes. A systematic comparison between approaches using CWT and short-time Fourier transform (STFT) is carried out. Simulated data are generated to test the performance of these methods when estimating time-frequency based coherence. Surprisingly and in contrast to the common belief, the coherence estimation based upon CWT does not always supersede STFT. We suggest that a combination of STFT and CWT would be most suitable for analysing non-stationary neural data. In both frequency and time domains, methods to test whether there are two coherent signals presented in recorded data are presented. Our approach is then applied to the electroencephalogram (EEG) and surface electromyogram (EMG) during wrist movements in healthy subjects and the local field potential (LFP) and surface EMG during resting tremor in patients with Parkinson's disease. A software package including all results presented in the current paper is available at http://www.dcs.warwick.ac.uk/~feng/software/COD.

Key words: Wavelet, Coherence, Confidence intervals, EEGs, EMGs, LFPs, time discrimination, frequency discrimination

1 Introduction

Coherence analysis has been extensively applied in studying the neural activity within nervous systems. Neurophysiological signals contain noise at all levels and are bound to be treated as random signals or stochastic processes [17]. A single stationary stochastic process is often characterised by its autocovariance function and its power spectrum. Power spectrum is the Fourier transform of the autocovariance function and provides us with the frequency description of the process. The frequency or spectral contents of such signals display important information and have been used to evaluate the physiological and functional state of the nervous systems. Fourier analysis has been used extensively in studying the spectra of neurophysiological signals and in recent years interests have been focused on the study of synchronised phenomena between two or more events, such as the synchronisation between brain areas [2, 31] and correlation between electroencephalogram (EEG), electromyogram (EMG) and magnetoencephalogram (MEG) [9, 21, 22, 7]. In general, the investigated signals or data are assumed to be stationary and the estimates of the individual and cross spectra are calculated to obtain the coherence estimate. Fourier analysis serves as the fundamental coherence estimation method which yields the informative periodograms. Based on Fourier analysis and under Gaussian assumption, confidence intervals of the estimated coherence can be estimated. The construction of the confidence intervals is of vital importance since it allows the significant correlation to be detected and statistically assessed at various frequency ranges.

A wide range of signals encountered in biomedical applications and nervous systems fall into the category of non-stationary signals whose statistical properties constantly change with time. Such non-stationarity makes the Fourier analysis limited when temporal information of how the signals' frequency components evolve with time is necessary to be looked at. Short-time Fourier transform (STFT), a method which applies a short time window to the signal and performs a series of Fourier transforms within the window as it slides across all the times, can overcome the problems brought by Fourier analysis and form a time-frequency representation of the signals

of interest. Alternatively, the wavelet transform provides a useful approach in investigating non-stationary signals, which is usually regarded as an "optimal" solution to the time and frequency resolutions. The wavelet analysis has previously been used to study the EEG [29, 14, 30, 33] and EMG [26, 12]. Recently, transform methods based on Fourier and wavelet analysis are compared in [3] in the application of neural data. In order to evaluate the interactions within the nervous system, such as the events of sensory stimulus and motor response, the relationship between simultaneously recorded neural and muscular data needs to be studied. To characterise and detect the rhythms between two random processes, cross correlation and cross spectral methods can be employed. Correlation detection based on wavelet transforms has been used in wind engineering [8] and climatic and oceanic research [36]. In recent years in connection with neurophysiological applications, cross spectrum and coherence analysis have been used to analyse spike activity [25, 15].

The main contribution of our paper is the following. First, When it comes to examine the relationship between two channels of signal recordings with multiple trials, a time-frequency coherence based on continuous wavelet transform (CWT) is proposed and the way of estimating its confidence intervals is described. Second, via extensive simulations and in contrast to most results presented in the literature that CWT has an obvious advantage over short-time Fourier transform (SFFT), we find that SFFT performs better than CWT to detect low frequency signals, and CWT works better for high frequency signals. Intuitively, this reflects the different intrinsic properties of SFFT and CWT. At a low frequency (more stationary signals), CWT which has a high nonlinearity than SFFT and is bound to perform worse. But at a high frequency, SFFT becomes less sensitive to signals. Based upon our results, we then suggest that a more reasonable approach to detect the coherence between two signals would use both SFFT and CWT rather than use CWT alone. Third, purely in terms of a time or frequency resolution, it is found that CWT usually outperforms SFFT, in agreement with results in the literature. Methods on how to statistically detect signals with different frequencies (frequency discrimination) or whether there is a time gap (time discrimination) between signals are introduced.

Our approach is then successfully applied to experimental data: EEG-EMG obtained from healthy subjects during a voluntary wrist movement task and LFP-EMG obtained from Parkinson's disease patients during involuntary resting tremor. In summary, results presented here involve in how to statistically deal with three key quantities in a time-frequency approach: magnitude, frequency and time, when multi-trials physiological data are available. We expect that our approach could reveal some fundamental facts when more massive data, for example, the LFPs recorded in a multi-electrode array are available [11, 4, 34].

2 Methods

2.1 Coherence magnitude

2.1.1 Continuous Wavelet Transform (CWT)

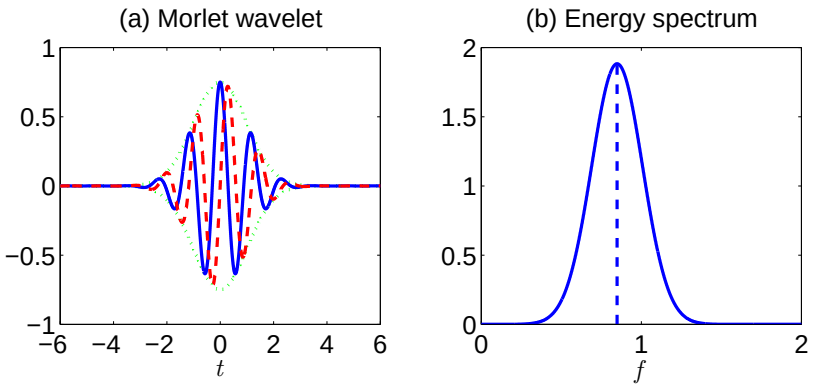

Figure 1: Morlet wavelet and its Fourier transform, $f_0 = 0.849$. (a) Morlet wavelet. The solid line is the real part and the dashed line is the imaginary part. The dotted line is the envelope. (b) Fourier transform of Morlet wavelet, with the vertical dashed line corresponding to the characteristic frequency f_0.

The continuous wavelet transform (CWT) of $x(t)$ is defined as

$$CWT_x(a,b) = \int_{-\infty}^{\infty} x(t)\psi^*_{a,b}(t)\,dt \tag{1}$$

where

$$\psi_{a,b}(t) = \frac{1}{\sqrt{a}}\psi\left(\frac{t-b}{a}\right) \tag{2}$$

$\psi(t)$ is called the mother wavelet where a is the dilation parameter, b is the location parameter and $*$ denotes complex conjugate. The choice of the wavelet should satisfy a number of selection criteria, such as the candidate functions having finite energy and satisfying admissibility condition [1].

The CWT is usually presented as a time-frequency representation by converting the scale parameter to the frequency. To fulfill this representation, a character frequency f_0 which is defined as the bandpass centre or central frequency of the wavelet energy spectrum is chosen and by use of the relationship between the converted frequency and arbitrary scale $f = f_0/a$ [1], the CWT can be expressed as

$$CWT_x(\tau, f) = CWT_x(a, b)|_{a=\frac{f_0}{f}, b=\tau} = \sqrt{\frac{f}{f_0}} \int_{-\infty}^{\infty} x(t)\psi^*\left(\frac{t-\tau}{f_0}\, f\right) dt \tag{3}$$

One of the most commonly used wavelets in practice is the Morlet wavelet, defined as

$$\psi(t) = \frac{1}{\pi^{1/4}}(e^{j2\pi f_0 t} - e^{-(2\pi f_0)^2/2})\, e^{-t^2/2} \tag{4}$$

where f_0 is the central frequency of the wavelet. If the choice of f_0 is appropriate the second term in the bracket which is known as the correction term becomes negligible, thus giving a simple Morlet wavelet [20]

$$\psi(t) = \frac{1}{\pi^{1/4}}\, e^{j2\pi f_0 t} e^{-t^2/2} \tag{5}$$

This expression shows that Morlet wavelet is a complex sine wave within a Gaussian envelope. The Fourier transform of the Morlet wavelet is

$$\hat{\psi}(f) = \pi^{1/4}\sqrt{2}\, e^{-\frac{1}{2}(2\pi f - 2\pi f_0)^2} \tag{6}$$

which has the form of a Gaussian function centred at f_0 with f_0 determining the wave numbers within the envelope and in practice the value of 0.849 is often used. In Fig. 1 a Morlet wavelet with $f_0 = 0.849$ and its Fourier transform are shown.

By employing the convolution theorem the wavelet transform can be expressed as the product of the Fourier transforms of the signal and wavelet, $\hat{x}(f)$ and $\hat{\psi}(f)$

$$CWT_x(a,b) = \sqrt{a}\int_{-\infty}^{\infty} \hat{x}(f)\hat{\psi}^*(af)e^{j2\pi fb}\,df \tag{7}$$

This relationship provides a convenient way when implementing CWT on computer since the Fourier transform of the wavelet function $\hat{\psi}_{a,b}(f)$ is already known in analytic form. The computation only requires an FFT of the original signal and an inverse FFT of the product of $\hat{x}(f)$ and $\hat{\psi}^*(af)$.

The square modulus of the wavelet transform is called the scalogram and is defined as

$$SCAL_x(\tau, f) = |CWT_x(\tau, f)|^2 \tag{8}$$

The scalogram is a time-varying spectral representation which describes the energy distribution of the signal. The scalogram $|CWT_x(\tau, f)|^2$ is often referred to as the wavelet spectrum. This is sometimes multiplied by a constant factor to give a slightly different expression [35, 1]. The wavelet spectrum gives a time-frequency representation, and it measures the contribution to the total energy coming from the vicinity of a point at a specific time and frequency for a given mother wavelet [23].

Another commonly used time-frequency representation is short-time Fourier transform (STFT) [28], defined as

$$STFT_x(\tau, f) = \int_{-\infty}^{\infty} x(t)w(t-\tau)e^{-j2\pi ft}\,dt = \int_{-\infty}^{\infty} x(t)w^*_{t,f}(t)\,dt \tag{9}$$

where $w^*_{t,f}(t) = w(t-\tau)e^{-j2\pi ft}$. STFT analyses the signal $x(t)$ through a short-time window $w(t)$: $x(t)w(t-\tau)$, and then a Fourier transform is performed on this product using a set of basis functions. The square modulus of STFT is referred to as the spectrogram

$$SPEC_x(\tau, f) = |STFT_x(\tau, f)|^2 \tag{10}$$

In this report, both CWT and STFT are used for the coherence analysis and the performance of the two is discussed in detail.

2.1.2 Time-Frequency Coherence

In order to study the relationship between two non-stationary processes definitions of cross spectrum and coherence are desirable. Given two processes $x(t)$ and $y(t)$ with their time-frequency representations $X(\tau, f)$ and $Y(\tau, f)$, the time-frequency cross spectrum between them is defined as

$$S_{xy}(\tau, f) = X(\tau, f)Y^*(\tau, f) \tag{11}$$

and the auto spectra are given by

$$S_x(\tau, f) = |X(\tau, f)|^2 \tag{12}$$

$$S_y(\tau, f) = |Y(\tau, f)|^2 \tag{13}$$

In the above equations, the $X(\tau, f)$ and $Y(\tau, f)$ can be based on either STFT or wavelet transforms. The time-frequency based coherence, the square of the cross spectrum normalised by the individual auto spectra, is defined by

$$R^2_{xy}(\tau, f) = \frac{|S_{xy}(\tau, f)|^2}{S_x(\tau, f)S_y(\tau, f)} \tag{14}$$

The above definitions are straightforward and they follow a similar approach to the Fourier analysis. In the Fourier analysis, the spectra and the coherence can be estimated by virtue of the periodogram method in which a number of segments are averaged to obtain the estimation. However, in the case of time-frequency coherence problems arise when using averaging because there are two dimensions of both time and frequency. It is unclear along which direction the smoothing should be done [35]. As noted in [35], the coherence will have an identical value of one at all times and frequencies without smoothing. In [8], a localised window T based on the time resolution is introduced to overcome this problem, however the choice of T is arbitrary and can suffer from a lack of interpretation. In [13], the wavelet coherence is analysed and the size of the smoothing window is chosen according to the oscillation cycles within the window. However, this wavelet coherence is based on single-trial brain signals. Here in the present report, a series of repeated trials are recorded and a consistent relationship between two signals needs to be explored. In this connection a smoothing

scheme based on the repeated trials is proposed and the estimate of the coherence is defined as

$$\hat{R}^2_{xy}(\tau, f) = \frac{|\hat{S}_{xy}(\tau, f)|^2}{\hat{S}_x(\tau, f)\hat{S}_y(\tau, f)} \tag{15}$$

where

$$\hat{S}_x(\tau, f) = \frac{1}{K}\sum_{k=1}^{K} |X_k(\tau, f)|^2 \tag{16}$$

$$\hat{S}_y(\tau, f) = \frac{1}{K}\sum_{k=1}^{K} |Y_k(\tau, f)|^2 \tag{17}$$

$$\hat{S}_{xy}(\tau, f) = \frac{1}{K}\sum_{k=1}^{K} X_k(\tau, f)Y_k^*(\tau, f) \tag{18}$$

The above equations (15)-(18) outlines the procedure for estimating the time-frequency coherence. The two channels of data contain a series of repeated trials $\{x_1(t) \dots x_K(t)\}$ and $\{y_1(t) \dots y_K(t)\}$ that are recorded simultaneously. In each trial $x_k(t)$ and $y_k(t)$, the time-frequency representations $X_k(\tau, f)$ and $Y_k(\tau, f)$ are calculated and their squared magnitude $|X_k(\tau, f)|^2$ and $|Y_k(\tau, f)|^2$ (spectrogram or scalogram) as well as the cross spectrum $X_k(\tau, f)Y_k^*(\tau, f)$ are calculated. After averaging across these multiple trials, the estimates for auto spectra and cross spectrum are obtained and they lead to the estimate of the time-frequency based coherence as expressed in (15). The average cross spectrum and its single-trial version consist of complex values, and the amplitude and phase spectra can be defined as the absolute value and angle respectively.

2.1.3 Confidence Intervals

In order to construct confidence intervals for the above time-frequency coherence some basic assumptions about the investigated time series or stochastic processes must be made. In Fourier analysis, the two time series are assumed to be stationary and a theoretical distribution (e.g. Gaussian) is used to approximate the probability density of the data.

However, because the time-frequency analysis contains temporal changes or time-varying information, the description of the statistics is confined to a localised interval

[27]. The wavelet spectra has been compared to Fourier spectra in [23] and the variance of the wavelet spectrum was analysed in [24]. The wavelet spectrum based on continuous wavelet transform was studied in [16]; where it was concluded that the wavelet spectrum can represent the second-order statistical properties of random processes for stationary and some non-stationary processes. It was shown that the local wavelet spectrum follows the mean Fourier spectrum [35]. Based on this assumption, the wavelet power spectrum should be χ^2 distributed and confidence levels for the cross-wavelet spectrum can be derived from the square root of the product of two χ^2 distributions.

For the setting of confidence intervals for the time-frequency based coherence the notion of generalised coherence is used here [6].

Let $\mathbf{X} = \{X_k(\tau, f)\}_{k=1}^K$ and $\mathbf{Y} = \{Y_k(\tau, f)\}_{k=1}^K$ denote the complex time-frequency representation of a sequence of repeated trials. Then the estimate of the coherence in (15) can be denoted by

$$\begin{aligned} \hat{R}_{xy}^2(\tau, f) &= \frac{|\langle \mathbf{X}, \mathbf{Y} \rangle|^2}{\|\mathbf{X}\|^2 \cdot \|\mathbf{Y}\|^2} \\ &= \frac{\left| \sum_{k=1}^K X_k(\tau, f) Y_k^*(\tau, f) \right|^2}{\sum_{k=1}^K |X_k(\tau, f)|^2 \cdot \sum_{k=1}^K |Y_k(\tau, f)|^2} \end{aligned} \tag{19}$$

where $\langle \mathbf{X}, \mathbf{Y} \rangle$ is the inner product of $\mathbf{X}$ and $\mathbf{Y}$, defined by

$$\langle \mathbf{X}, \mathbf{Y} \rangle = \sum_{k=1}^K X_k(\tau, f) Y_k^*(\tau, f) \tag{20}$$

$\|\mathbf{X}\|^2 = \langle \mathbf{X}, \mathbf{X} \rangle$ and $\|\mathbf{Y}\|^2 = \langle \mathbf{Y}, \mathbf{Y} \rangle$ are the squared magnitudes of $\mathbf{X}$ and $\mathbf{Y}$. The time-frequency based coherence takes the values between 0 and 1 and in particular, $\hat{R}_{xy}(\tau, f) = 0$ if $\mathbf{X}$ and $\mathbf{Y}$ are orthogonal, if $\mathbf{X} = a\mathbf{Y}$ for any non-zero complex number a then $\hat{R}_{xy}(\tau, f) = 1$.

If the two processes are independent the coherence is particularly useful because no common signal component is present. Under the hypothesis that the two processes are independent Gaussian noise it allows thresholds corresponding to a particular probability of false alarm to be set directly. The distribution of the coherence estimate

[6] is given by

$$\Pr(R^2 \leq r) = 1 - (1-r)^{K-1}, \quad 0 \leq r \leq 1 \tag{21}$$

where $P(\cdot)$ denotes the probability, and r is the detection threshold. For a confident interval of probability 0.95, $1 - (1-r)^{K-1} = 0.95$, and the detection threshold is $r_{95\%} = 1 - 0.05^{1/(K-1)}$. This says that the estimate which is less than this value should be regarded as insignificant.

The above construction of the confidence interval is based on the assumption that the two processes have independent Gaussian distribution. However, as pointed out in [5], the distribution of the coherence estimate does not depend on the statistics of one of the two processes provided that the other process is Gaussian and the two processes are independent. This property shows that the coherence estimate is invariant with respect to the second channel statistics as long as one of the two independent processes is Gaussian. This assumption can be further weakened by a geometric argument that the process has spherically symmetric distribution (see Appendix A) instead of the stronger Gaussian assumption [5, 32].

2.2 Discrimination in frequency domain

The time-frequency coherence analysis gives out a result in both the time and frequency domain. Usually the result is illustrated through a graphic plot in the dimensions of time and frequency, thus a direct visual examination can reflect the correlated components in the joint time-frequency plane. However, as for the non-stationary signals, whichever approach either CWT or STFT is used, it is necessary to use statistical methods to assess the frequency discrimination of both methods. More exactly, assume that we find the maximum values of the coherence at two frequencies f_1 and f_2, $f_2 \neq f_1$, we want to statistically test whether $f_1 \neq f_2$ or not.

The test for the frequency discrimination is important since it tells us the ability of the coherence estimator to separately discriminate two correlated components that are close in frequency. From this point, we can fix a frequency f_1 where the two processes are correlated at a given time interval, and then calculate the maximum

coherence value $R(f_1)$ at this frequency f_1. For a nearby frequency f_2 we can compute its maximum coherence value $R(f_2)$. To test the frequency discrimination at these two adjacent frequencies, we can generate enough testing data sets and derive the density functions of $R(f_1)$ and $R(f_2)$: $g_1(f)$ and $g_2(f)$. To see if f_2 can be discriminated from f_1, we can choose an observation value $F = f_0$ where $g_1(f_0) = g_2(f_0)$ and use the following error probability as the discrimination criterion

$$\Pr(F \geq f_0 \mid g_1) = \alpha \tag{22}$$

If a 5% error probability is selected, i.e. when $\alpha < 0.05$ we can say that the nearby frequency f_2 can be discriminated from f_1.

How to tell one signal from another when noise is presented is a fundamental issue in statistics. In classical statistics, two signals are separable as soon as noise vanishes. Here, however, we are dealing with a totally different situation. From the uncertainty principle, we know that even without noise, we have difficulty to distinguish between two signals in time or frequency domain.

2.3 Discrimination in time domain

In this section, we aim to elaborate on the issue of time discrimination for the time-frequency coherence using both STFT and CWT. Unlike the frequency discrimination in which we can fix one frequency and see how close the nearby frequency can approach the first fixed one until the second frequency cannot be identified, the coherence in the time dimension is usually reflected as correlation during a time interval. It is difficult to fix one interval and test the other nearby one since they can be chosen randomly with each spanning different widths. Conversely, for a given frequency we can choose two processes correlated across the entire time range but with a small period of the same time interval in each process having no correlation at all. The width of this gap period in the coherence analysis indicates the time discrimination ability and the narrower the gap is, the better time discrimination result we will have.

Since the two processes have no correlation only in the gap interval, the coherence

estimate at the chosen frequency will have a significant dip around the chosen gap but remain high amplitudes on the both sides of the dip. When the gap disappears the coherence will jump back to the high amplitude around the original dip and hold this amplitude for the entire time. Hence, one can calculate the distance between the minimum coherence value at the dip and the neighbouring values where the coherence jumps to the maxima. When the size of the gaps are reduced, we can see how narrow the gap can reach until the coherence estimate can not distinguish the minimum and maximum value of the dip, i.e. those two values are too near to be discriminated.

When the maximum and minimum values from the sample data are available, one can obtain the distributions of the two quantities. A statistical test can be used to test if these two maximum and minimum values are equal, e.g. t-test.

3 Results

3.1 Simulated data

In order to test the performance of the time-frequency coherence defined above, artificial data was generated to simulate the processes containing repeated trials. The two test time series are Gaussian white noise with sine waves embedded in each trial of the two processes. The signal-to-noise ratio (SNR), which is the logarithm ratio of the power of the sine wave and the power of the white noise, is set to be -10 dB, -15 dB and -20 dB. The Gaussian white noise used here have unit power and the amplitudes of sine wave in each trial are adjusted according to the value of SNR to satisfy the SNR settings.

Figure 2 shows a typical three-dimensional plot of the time-frequency coherence defined above and in this example only the coherence using CWT is given as illustrating the general idea of the coherence distribution in both time and frequency. The SNR was chosen as -10 dB and 20 trials were used. The plane in the figure shows the 95% confidence interval calculated based on (21). The sine waves with 25 Hz were embedded into the white noises from 500 ms to 600 ms in each trial of both white

noises. A significant peak can be seen in the estimates of both the STFT and wavelet coherence between 500 ms and 600 ms and around 25 Hz in the time-frequency plane. This illustrates clear correlation over specific ranges of time and frequency.

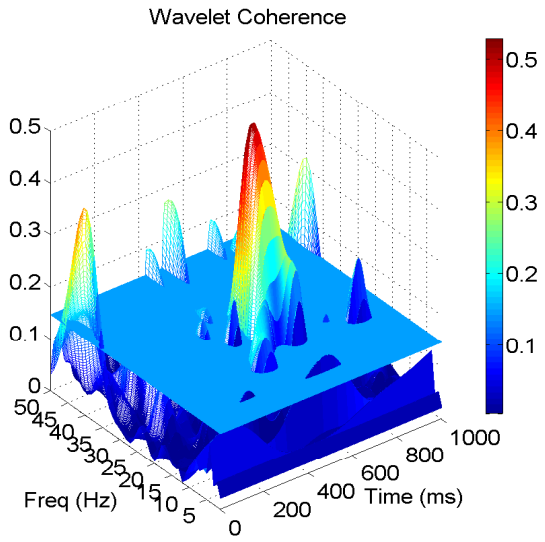

Figure 2: Time-frequency coherence using CWT of two Gaussian white noises of 1000 ms with two sine waves of 25 Hz which were embedded from 500 ms to 600 ms in each channel. The SNR was set to be -10 dB and 20 trials were generated with sampling rate 1 kHz. Morlet wavelet was used with $f_0 = 0.849$.

In Fig. 3, time-frequency coherence estimates are shown using two different time-frequency representations STFT and CWT under two SNR settings, -15 dB and -20 dB. The numbers of trials here were 50 and 200 for -15 dB and -20 dB, respectively. For different SNRs, the number of trials was also chosen to be different in order to detect the correlation under lower SNR settings. The results will improve if more trials are used in the estimation. In general the two methods could successfully resolve the correlation at both the three different time intervals in which three signal components are embedded and the three different frequencies under low SNR settings. The window length in the STFT was 300 ms, if a shorter window was used the results gave a good time resolution but the frequency resolution became poor. This reflects the trade off between time and frequency resolution inherent in the STFT method. The wavelet

coherence, using a complex Morlet wavelet, achieves to give a compromised result between time and frequency resolution. The wavelet transform analyses the high frequency parts with better time resolution and low frequency part with poorer time resolution. Compared to the fixed time-frequency resolution for each frequency in STFT, the wavelet analysis holds this demanding property. Both the STFT and wavelet satisfy the uncertainty principle and are bounded by the Heisenberg box in the time-frequency domain [1]. For the simulation result of the test data here which contains three different frequency components 5 Hz, 25 Hz and 40 Hz, STFT gives a better resolution than CWT at the low 5 Hz frequency, while CWT performs better for the higher 25 and 40 Hz frequencies. When the two methods are applied to more test data, it holds the result that STFT performs better than CWT at the low frequencies but gives a poorer result at the higher frequencies (see Fig. 4). It is readily seen from Fig. 4 that when the frequency is below 12 Hz, the coherence calculated based on STFT is higher than that of CWT. In other words, the low frequency coherence is more easily detected using STFT than CWT. This shows that a reasonable way to analyse the coherence is to average out the pros and cons of the two. Our results are then tested for a wide range of SNR settings (not shown here).

Fig. 4 also tells us another two interesting issues: time and frequency discrimination for both methods. Bottom two right figures of Fig. 4 basically say that a much better frequency resolution is achieved when the coherence frequency is high (say > 10 Hz). For time resolution (top two right figures of Fig. 4), it is difficult to draw a conclusion intuitively. In the next two subsections, we discuss and compare the frequency discrimination and time discrimination of the two methods in details based on our statistical test methods.

3.2 Test on frequency discrimination

In fact, a closer look at Fig. 4 bottom right reveals some interesting features for CWT and STFT analysis. At a low frequency (≤ 10 Hz), for STFT the coherence reaches its maxima between 0 and 1 Hz, despite the fact that the true coherence should be at $1, 2, \cdots, 10$Hz. In other words, the frequency resolution is very low at a

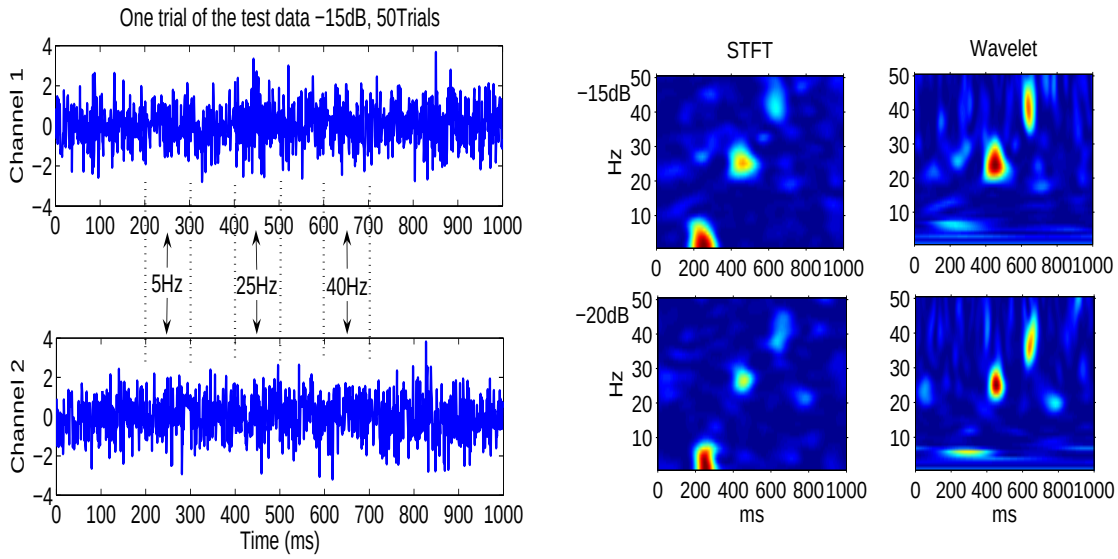

Figure 3: Time-frequency coherence using STFT and wavelet CWT under two different SNRs of -15 dB and -20 dB. Three sine wave components with different frequencies were embedded into the Gaussian white noises in each trial at 200-300 ms with 5 Hz, 400-500 ms with 25Hz and 600-700 ms with 40 Hz. Different trials were generated for different SNRs with sampling rate 1 kHz, 50 trials at -15 dB and 200 trials at -20 dB. In the figure, the left column used STFT and the right column used the CWT. From the top to the bottom, the SNR was set to be -10 dB and -15 dB, respectively. In the STFT, the Gaussian data window of width 300 ms was used. The CWT used Morlet wavelet with $f_0 = 0.849$.

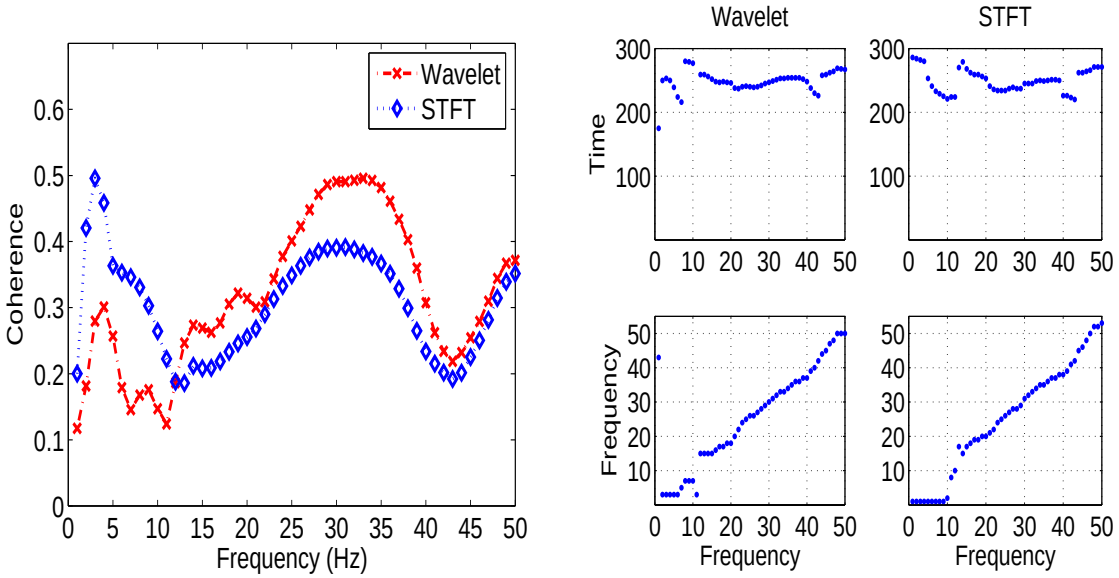

Figure 4: (Left): Use one white noise series, length 500 ms, with only a single period of sine waves embedded, from 200 ms to 300 ms. The sine waves are selected to have the frequencies from 1 Hz to 50 Hz and the coherence is calculated for each frequency as it moves from 1 to 50 Hz in order to compare the two methods for all these frequencies. The amplitude of the STFT coherence is adjusted to have the same maximum height as CWT to allow for a uniformed scale for the comparison of the two. A critical frequency at around 12 Hz is clearly shown. (Right): The data used is the same as above: the test data consists of 500 ms white noise and a single period of sine waves are embedded from 200 to 300 ms with the frequencies moving from 1 Hz to 50 Hz at which frequency the coherence is calculated and the maximum value is obtained for each frequency. It shows that at which time and frequency the coherence of STFT and CWT reach its maximum value. Generally speaking, both methods can pick up these correlations at the frequencies and time intervals where the sine waves are added.

low frequency. This is also true for the case of CWT. How is the frequency resolution at a high frequency?

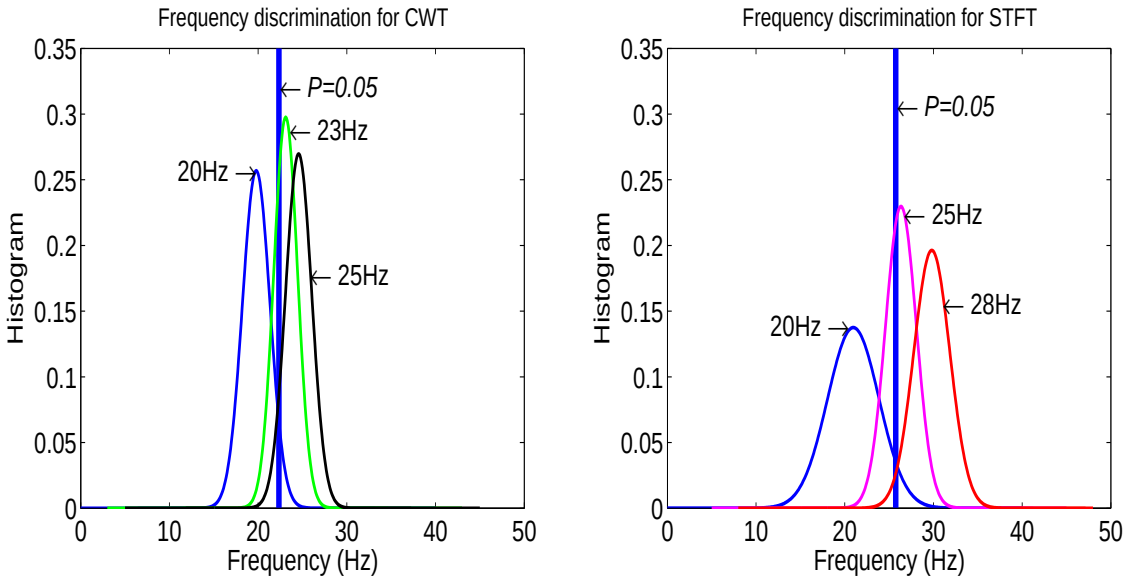

Figure 5: 100 independent sets of test data are generated (SNR -10 dB, Trials 20) for each histogram. The first frequency is chosen to be $f_1 = 20$ Hz. A 5% error probability was selected as the discrimination criterion, i.e. when the error is less than this value it can be said that the nearby frequencies f_2 can be discriminated from f_1. Form the figures, one can see that for STFT $f_2 = 28$ Hz, for CWT $f_2 = 26$ Hz.

To this end, we used our method for frequency discrimination and generated 100 independent sets of test data (SNR -10 dB, Trials 20). The first frequency was chosen to be fixed at $f_1 = 20$ Hz and the distribution of its maximum coherence value of the 100 sets is approximated by a normal distribution (see Fig. 5). A 5% error probability was selected as the discrimination criterion, i.e. when the error is less than this value it can be said that the nearby frequencies f_2 is different from f_1. For a given frequency f_2, 100 independent samples of the maximum coherence value were generated again and is approximated by another normal distribution. From Fig. 5 one can see that for STFT the critical frequency is around $f_2 = 28$ Hz, but for CWT it is $f_2 = 25$ Hz. Hence if we observe that one coherence arrives at its maximum value at 20 Hz, and the other attains at 26 Hz for CWT analysis, we can assess there are two signals

with different frequencies, with a probability of 95%. For STFT analysis, we require that the other signal should be with a frequency higher than 28 Hz so that we could statistically discriminate between them.

As we mentioned, for the frequency result in Fig. 4 both STFT and CWT indicate a very coarse frequency resolving ability under 10 Hz in the low frequency range. To show the frequency discrimination in this range, we plot the discrimination results for the frequencies from 1 Hz to 10 Hz in Fig. 6. Unlike the clear discrimination result given at the frequency of 20 Hz, it is generally difficult to say if one frequency can be discriminated from the others in the low frequency range < 10Hz for both CWT and STFT. In the CWT result, the frequency distribution at 1 Hz is not shown because the mean frequency for the 100 tests is around 20 Hz which is significantly biased. However, if specifying a fixed frequency at 5 Hz we can still discriminate the nearby frequencies from 8 Hz onwards. For the STFT result we can hardly find any discriminated frequencies from each other since their distributions are all centred around certain frequencies between 1 and 5 Hz. The frequency distributions at 3 Hz, 4 Hz and 5 Hz are not shown because the distribution for these three is a delta function at 1 Hz for all 100 samplings.

3.3 Test on time discrimination

Using the test method for the time discrimination in section 2.3, again 100 samples are generated for time gaps of 5, 10, 20 and 50 ms. The average results for both methods are shown in Fig. 7 bottom two panels. It is seen that CWT has a narrower strip in frequency domain than STFT, in agreement with what we claimed in the previous subsection. However, from the average results, one might conclude that STFT has a higher resolution in time than CWT. When the time gap is only 5 ms, we could see there is a small dip in STFT coherence, but it is almost flat for CWT. When the time gap is 50 ms, the coherence obtained from STFT approach is discontinuous, but not for CWT.

To statistically confirm our conclusions, we then plot the coherence vs. time when the frequency is fixed at 20 Hz in Fig. 7 upper panel left. The t-value is read out

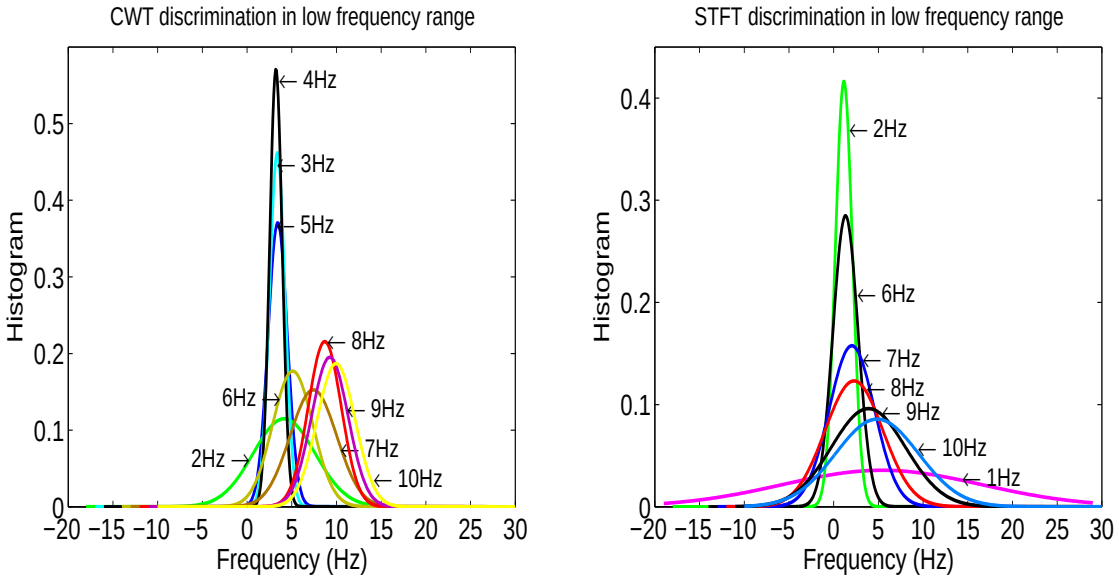

Figure 6: Frequency discrimination in the low frequency range from 1 Hz to 10 Hz: 100 independent sets of test data are generated (SNR -10 dB, Trials 20) for each histogram. 100 independent sets of test data are generated (SNR -10 dB, Trials 20) for each histogram. Left, CWT method and frequency at 1 Hz is not shown; Right, STFT method and frequencies at 3 Hz, 4 Hz and 5 Hz are not shown.

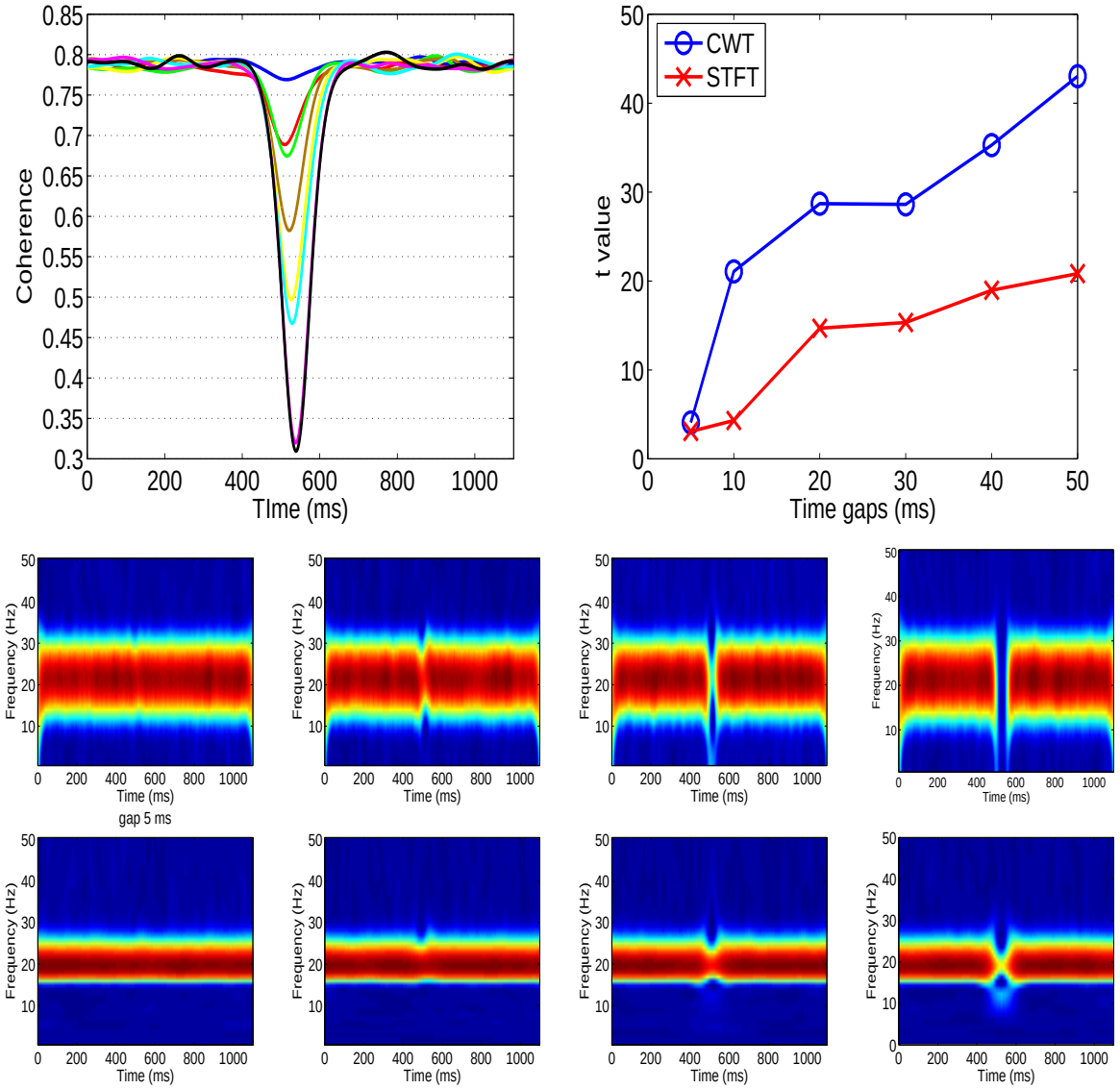

Figure 7: Top left, coherence averaged across 100 samples using CWT with a fixed frequency at 20 Hz and the eight lines delving in the middle with different depths from the top to the bottom correspond to the time gaps from 10 ms to 80 ms (see figures at bottom and middle panels). Top right, calculated t-value as described in the text. Middle panel, averaging coherence in frequency-time domain for STFT. Bottom panel, averaging coherence in frequency-time domain for CWT. From the left to the right, four columns correspond to the time gaps of 5, 10, 20 and 50 ms

from carrying out t-test for the maximum and minimum coherence values around the time gaps. Surprisingly we found that the t-test gives us completely different results. Fig. 7 upper panel right clearly indicates that again CWT is better than STFT: all t-values obtained from CWT are higher than STFT, although the results tell us that both methods have rather high time resolution. With a time gap of 5 ms, we are still able to tell if there are two signals presented or not.

3.4 Data with unmatched sine waves

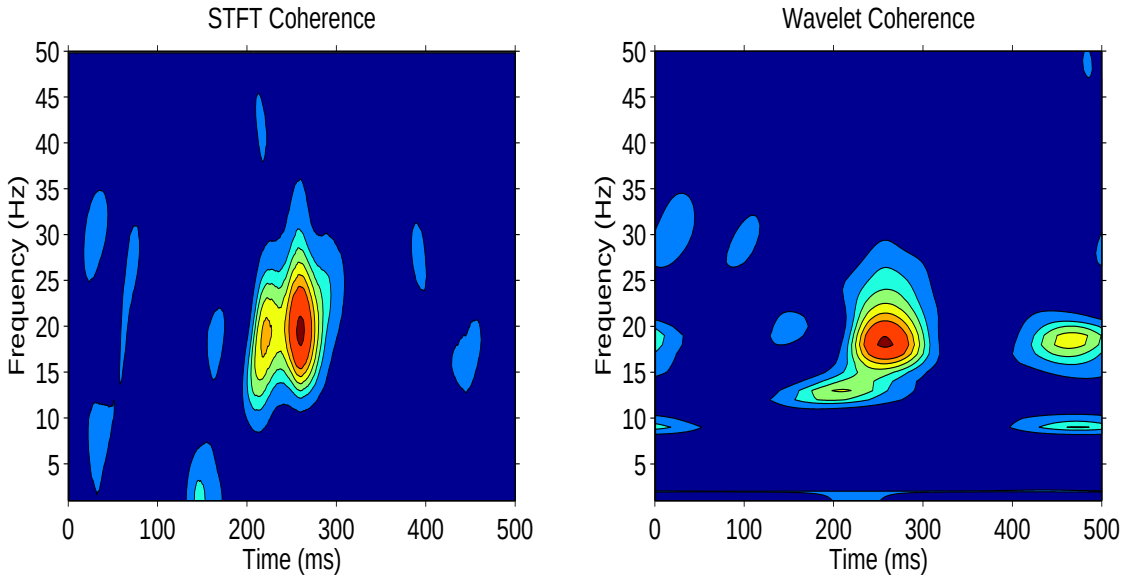

Figure 8: Coherence analysis with unmatched sine wave in each trial of the two channels of test data. The data consists of 20 trials with SNR -10 dB and unmatched sine waves are embedded into 200-300 ms interval of the 500 ms length in each trial. The choice of the analysing window for STFT and wavelet for CWT is the same as in the simulated data. Regions above the 95% confidence interval are shown. Left: STFT method; Right: CWT method.

The above simulated data are generated using the sine waves which are symmetrically embedded into every single trial of each channel. In real applications, this may not be the case because the harmonious components in each trial are unlikely to be homogeneous although recordings come from repeated trials. In order to test

the influence of the inhomogeneity in each trial, unmatched sine waves are used in each trial. In one channel 25% of the total sine waves in each trial are taken out randomly while the other channel remain the same with no sine waves taken out. For the results shown in Fig. 8, the sine waves have the frequency of 20 Hz with the SNR setting -10 dB and trial number 20. The coherence from the both methods reaches the correlation at 20 Hz between 200-300 ms in which the sine waves are embedded. However, for the CWT coherence, there appears other less significant peaks at other frequencies and time intervals. It suggests that inhomogeneity can create other coherence values which are not presented in the signals using the CWT method, though this inhomogeneity is less prominent in the STFT method.

3.5 Application to Neural and Muscular Signals

3.5.1 Movement-related signals

As an illustration of the above time-frequency coherence, an example with application to neural signals is given in this section. The data that contains simultaneously recordings of EEG and EMG was collected during the voluntary movements of wrist extension/flexion. The two pair of EEG electrodes were placed 2.5 cm lateral to the vertex (Cz) with spacing 2.5 between each other while the EMG electrodes were attached to the extensor forearm muscle [9]. The subjects repeatedly perform moving and holding movements between the extension and flexion positions. Fig. 9 left shows a period of EEG and EMG signals recorded from subjects' performing such wrist moving and extending movement. In this figure, 0-1.5 s is the is the moving period when the wrist start moving towards extension position and 1.5-3.5 s is the maintaining period when the wrist holds at the extension position. Before taking the coherence analysis, both channels of data are preprocessed to have their mean subtracted and trend removed, and for the EMG a full wave rectification is applied.

Wavelet coherence analysis of EEG and EMG signals during wrist moving and extending periods is shown in Fig. 9. Forty repeated trials of moving and extending movement were included. The subjects followed the auditory cues which were used

as the trigger time to signal the start of the extension phase. In each trial the total 3.5 s movement involves the moving period which is from 0-1.5 s and the maintaining period which is from 1.5-3.5 s. The wavelet coherence displays a dominant peak appears during the maintaining period at 2.8 s and 20 Hz with coherence value 0.29 as well as two other distinct components at 2.5 s, 20 Hz and 3.0 s, 21 Hz, respectively; the STFT method reveals the maxima of the coherence at 2.8 s which has the same time instant as in the wavelet analysis and the frequency position is 22 Hz. There are also two peaks at 2.3 s and 3.2 s with at the frequency of 20 Hz and this gives similar result to the wavelet coherence. This indicates strong correlation between the lateral EEG and extensor EMG during the maintaining period from 2.5 s to 3.0 s at the frequency of approximate 20 Hz. A closer look of the the coherence and phase spectrum at the frequency of 20 Hz where the coherence reaches its maximum value also indicates a phase-locked phenomenon with opposite phase between the two EEG and EMG signals during the maintaining position.

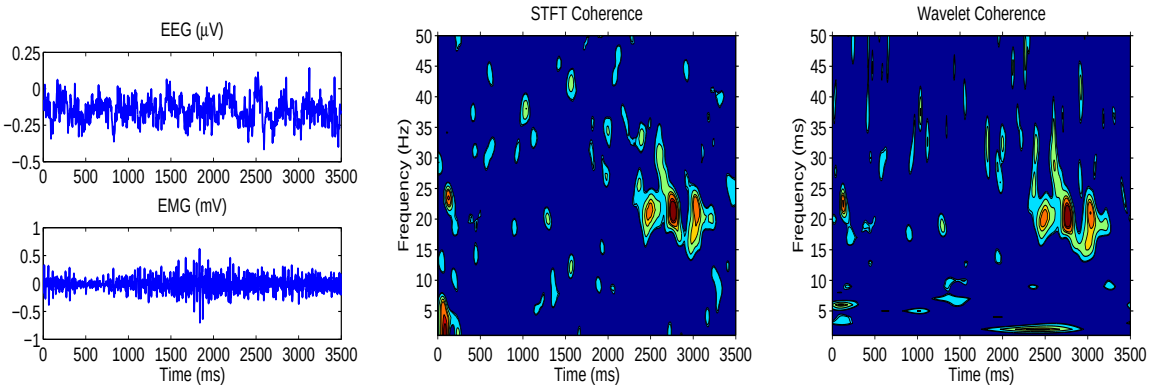

Figure 9: Coherence analysis using STFT and wavelet methods between EEG and EMG signals during the wrist performs moving and extending movements. The choice of the analysing window for STFT and wavlet for CWT is the same as in the simulated data. Only regions above the 95% confidence interval are shown.

Besides the above main correlations around 20 Hz during the maintained positions, the two time-frequency coherence methods identify prominent components during the time when the movement starts. In the low frequency band below 10 Hz, the STFT coherence shows a peak of value 0.25 at around 0.08 s and 4 Hz while wavelet

coherence shows a peak of value 0.19 at around 0.08 s and 0.6 Hz. This indicates the correlation occurs at the movement onset and STFT gives a larger coherence value than the CWT method in the low frequency range. Another correlation happens during this moving period is at the frequency of around 23 Hz with the time 0.1 s, and both the STFT and CWT methods yield the same level of coherence amplitude. The remaining peak that appears at the low frequency under 5 Hz around 2.5 s in the CWT method whereas is not presented in the STFT result may attribute to the unmatched oscillatory patterns in each trial or any disturbance which causes the difference across the trials during the recording. This reflects the inhomogeneity brought by the unmatched signal components investigated in Section 3.4.

From Fig. 9, we can see that there three major coherence components. For CWT, they are on the time of 2.5 s at 20 Hz, 2.8 s at 20 Hz and 3.0 s at 21 Hz. For STFT, they are 2.3 s at 22 Hz, 2.8 s at 20 Hz, and 3.2 s at 20 Hz. The SNR, calculated as the ratio of the power from 1-250 Hz and from 251-500 Hz, is < -10.2091 dB, hence our results given in the section of simulated data can be directly applied here. There are three broken and coherent signals in the coherence plot, suggesting that significant coherence appears in different time periods but it is unclear whether they are statistically independent in frequency.

3.5.2 Tremor-related signals

Deep brain stimulation is regarded as an effective approach for the clinical treatment of Parkinson's disease and it also provides the opportunity to study neuronal activity recorded from the implanted electrode for chronic stimulations of subthalamic nucleus (STN)[18, 19]. As another example of the application of the proposed time-frequency coherence analysis, STN local field potentials (LFPs) and surface EMGs from the forearm extensor muscle were simultaneously recorded from Parkinson's disease patients during resting tremor were analysed here.

Fig. 10 shows a period of typical LFP and the EMG signals during the intermittent tremor as well as the time-frequency analysis of the two signals. The data has a recording of 66 s with sampling frequency 500 Hz and it was partitioned into 33

segments with 2 s in each trial. At a first glance, we can see that both the STFT and CWT coherence analyses indicate strong correlations in the low frequency range under the 10 Hz. There are also additional clear features at other frequencies. The CWT coherence reaches its maximum value of 0.22 at 20 Hz and 1.57 s, and around this position STFT has a peak of value 0.13 at 19 Hz and 1.58 s. The maximum value for STFT coherence is 0.21 at 12 Hz and 1.30 s, and around this position the CWT coherence has a peak of 1.19 at 11 Hz and 1.29 s. The CWT coherence also has a significant peak at 29 Hz and 0.59 s with the value of 0.21 while around this position the STFT shows a relatively small peak at 22 Hz and 0.67 s with the value of 0.14. This says a higher CWT coherence value at higher frequencies according to our previous analysis of the two. Other corresponding significant coherence for the two methods of CWT vs. STFT in 10-15 Hz frequency range is at the following positions: 0.29 s 14 Hz (Coherence: 0.15) vs. 0.26 s 15 Hz (Coherence: 0.14), 1.07 s 14 Hz (Coherence: 0.19) vs. 1.08 s 15 Hz (Coherence: 0.14).

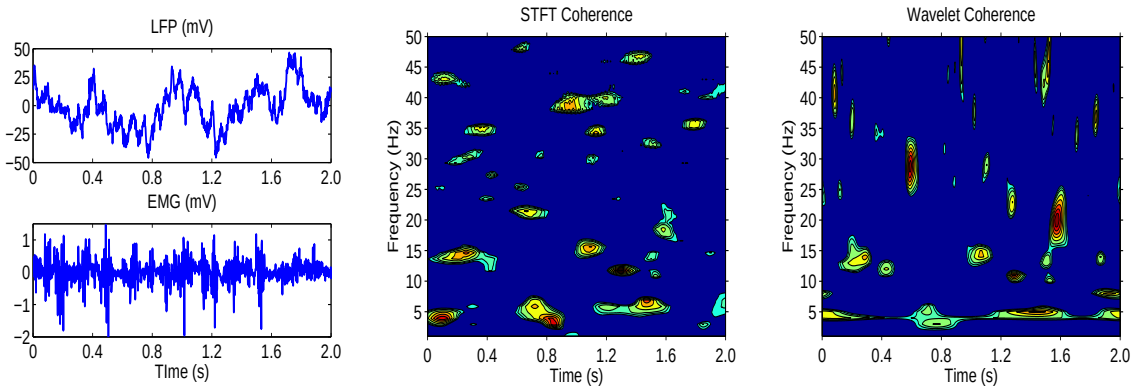

Figure 10: STFT and wavelet coherence of STN LFP and EMG signals for the Parkinson's disease patients and only regions above the 95% confidence interval are shown. The choice of the analysing window for STFT and wavlet for CWT is the same as in the simulated data.

If we look at the low frequency band under 10 Hz, there are three major significant peaks. For CWT they are at 0.01 s 5 Hz (Coherence: 0.13), 0.79 s 3 Hz (Coherence: 0.12) and 1.45 s 5 Hz (Coherence: 0.17); for STFT they are at 0.12 s 4 Hz (Coherence: 0.20), 0.85 s 3 Hz (Coherence: 0.20) and 1.47 s 7 Hz (Coherence: 0.17). At these low

frequencies, the coherence values estimated from STFT seem to be generally higher than CWT, confirming that at low frequency range of $<$ 10Hz STFT yields higher coherence values than CWT. However, for both CWT and STFT we can clearly see that strong correlations occur during the whole time course of 2.0 s at low frequency band of 3-7 Hz. Our results here are in accordance with the previous spectral findings from the recordings of Parkinson's disease patients[18, 10, 37]. Comparing this result and the one shown in the section of movement-related signals, very different mechanisms of neural and muscular synchronisation may exist between healthy subjects and Parkinson's disease patients.

4 Discussion

The neural data examined in the previous section was treated as non-stationary signals including two examples of EEG-EMG analysis during voluntary wrist movements of normal subjects and LFP-EMG analysis recorded from Parkinson's disease patients with tremor. From the results given by our time-frequency coherence analysis, it has proved that our approach can successfully detect the correlated synchronisations from the noisy electrophysiological signals hence it can serve as a useful tool when analysing the correlated relationship between two non-stationary signals.

The first EEG-EMG example found that synchronisations arise in the 15-30 Hz range, which is referred to as the β band in the cortical rhythm. In addition to this major frequency band, correlation was also detected during the onset of the movement phase with a low frequency around 5 Hz. The second example is the coherence between LFP and EMG. It shows that a continuous correlated synchronisation spanned over the whole time at low tremor and double-tremor frequencies ranging from 3 to 7 Hz. Time-frequency coherence can disclose how the correlation evolve with time, and this is of great importance for the analysis of time course with dynamic changes within the nervous systems and thus help understand the timing relationship.

The way to find the confidence interval is given. Since both STFT and CWT spectra are estimated by averaging of the spectrograms and scalograms in each trial,

averaging is important here and if without averaging coherence will be value 1 on the whole time-frequency plane because the individual spectra of the two processes from STFT and CWT are simply themselves if there is only one trial of data. The correlations between two non-stationary processes are detected from the repeated observations in each of which we assume that they follow a consistent pattern. If in each trial the signal components that are aimed to be detected tend to be lack of this homogeneity, additional peaks may appear at other places according to out results and this makes the interpretation difficult.

In the present study, we have assessed the frequency and time discrimination of our proposed time-frequency coherence analysis in detail. From the test of 100 independent sample sets of simulated data, we have shown that CWT method gives a better resolution than STFT for a chosen 20 Hz frequency when a 5% error probability is chosen as the criterion for whether two nearby frequencies can be discriminated. For the time discrimination, both methods can resolve the time gaps even when they are as narrow as 5 ms and this property indicates the very high time resolution brought by this time-frequency coherence analysis. The STFT method was found to have a worse time resolution than CWT as illustrated by the t-test of the minimum and maximum value around the gap dip for both methods, although a direct visual inspection would say that STFT is better than CWT. Statistical approaches to discriminate between two signals presented here are only for illustrative purposes, and it is obvious that similar approaches could be adopted to test other issues.

STFT has been extensively used in the application of non-stationary signals. STFT uses the fixed windows and is regarded less popular than the wavelet methods because of the trade-off between temporal and spectral resolution. However, our results here found this is not always the case. The comparison between the STFT and CWT clearly shows that under different SNR settings STFT coherence always gives a better result than the CWT coherence in the low frequency range using the CWT with Morlet wavelet and STFT with Gaussian window. In general, the time-frequency method based on CWT and STFT used here proves effective in the analysis of correlations in the time course and frequency positions, and it has been successfully applied

to the investigation of the interactions between neurophysiological signals such as EEGs, LFPs and EMGs. It is advised to evaluate both methods when analysing two non-stationary processes using time-frequency coherence.

Although the current study is confined to EEG, LFP and EMG data of single or double channel recordings, it is readily seen that our approach could be directly applied to data from *in vivo* multi-unit recordings. For multiple spike trains recorded from multi-electrode array, our approach is again directly applicable if the firing rates are taken into account.

Appendix: Spherically Symmetric Processes

Given a complex random processes denoted by $\{\mathbf{a} = x_n + i\, y_n\}_{i=1}^{N}$, if the probability density function of $\mathbf{a}$ can be expressed as

$$f_{\mathbf{a}}(x_1, \ldots, x_N, y_1, \ldots, y_N) = f_{ss}\left(\sum_{n=1}^{N}(x_n^2 + y_n^2)\right) \tag{23}$$

where f_{ss} is a one-dimensional function, i.e. the value of the density function depends only on the distance from the origin and not on the direction, then $\mathbf{a}$ is said to be spherically symmetric. For detailed discussion about the property spherically symmetric, one can refer to [5].

Acknowledgment. J.F. was partially supported by grants from UK EPSRC (GR/R54569), (GR/S20574), and (GR/S30443).

References

[1] Addision, P. (2002). The Illustrated Wavelet Transform Handbook. *IOP Publishing Ltd*

[2] Andrew, C. and Pfurtscheller, G. (1996). Event-related coherence as a tool for studying dynamic interaction of brain regions. *Electroenceph. Clin. Neurophysiol.***2**, 144-148.

[3] Bruns, A (2004). Fourier-, Hilbert- and wavelet-based signal analysis: are they really different approaches? *J. Neurosci. Meth.***137**, 321-332.

[4] Feng, J.F. (2004). *Computational Neuroscience: A Comprehensive Approach.* Feng, J.F. (Ed.), Chapman and Hall / CRC Press, Boca Raton.

[5] Gish, H. and Cochran, D. (1987). Invariance of the magnitude-squared coherence estimate with respect to second-channel statistics. *IEEE Trans Acoust , Speech, and Signal Processing*, **ASSP-35** 1774-1776

[6] Gish, H. and Cochran, D. (1988). Generalized coherence. *International Conference on Acoustics, Speech, and Signal Processing*, **5**, 2745-2748

[7] Grosse, P., Cassidy, M. and Brown, P. (2002). EEG-EMG, MEG-EMG and EMG-EMG frequency analysis: physiological principles and clinical applications. *Clin. Neurophysiol.* **113**, 1523-1531

[8] Gurley, G., Kijewski, T. and Kareem, A. (2003). First-and higher-order correlation detection using wavelet transforms. *J. Eng. Mech.* , **129**,188-201

[9] Halliday, D.M., Conway, B.A., Farmer, S.F. and Rosenberg, J.R. (1998). Using Electroencephalography to study functional coupling between cortical activity and electromyograms during voluntary contractions in humans. *Neuroscience Letters*, **241**,5-8

[10] Halliday, D.M., Conway, B.A., Farmer, S.F., Shahani, U., Russell, A.J.C. and Rosenberg, J.R.(2000). Coherence between low-frequency activation of the motor cortex and tremor in patients with essential tremor. *The Lancet*, **355**, 1149-1153

[11] Horton, P. M., Bonny, L., Nicol, A.U., Kendrick, K.M. and Feng, J.F. (2005). Applictions of multi-variate analysis of variances (MANOVA) to multi-electrode array data. *J. Neurosci. Meth.*, **146**, 22-41

[12] Karlsson, J., Östlund, N., Larsson, B. and Gerdle, B.(2003). An estimation of the influence of force decrease on the mean power spectral frequency shift of

the EMG during repetitive maximum dynamic knee extensions. *Journal of Electromyography and Kinesiology*, **13**, 461-468

[13] Lachaux, J., Lutz, A., Rudrauf, D., Cosmelli, D., Le Van Quyen, M., Martinerie and J., Varela, F. (2002). Estimating the time-course of coherence between single-trial brain signals: an introduction to wavelet coherence. *J Neurophysio Clin*, **32**, 157-174

[14] Lambertz, M., Vandenhouten, R., Grebe, R. and Langhorst,P. (2000). Phase transitions in the common brainstem and related systems investigated by non-stationary time series analysis. *Journal of the Autonomic Nervous System*, **78**, 141-157

[15] Lee, D. (2002). Analysis of phase-locked oscillations in multi-channel single-unit spike activity with wavelet cross-spectrum. *J Neuro Meth*, **115**, 67-75

[16] Li, T. and Oh, H. (2002). Wavelet spectrum and its charaterization property for random processes. *IEEE Trans Inform Theory*, **48**, 2922-2937

[17] Lin, Z. and Chen, J (1996). Advances in time-frequency analysis of biomedical signals. *Critical Reviews in Biomedical Engineering* **24**, 1-72.

[18] Liu, X., Ford-Dunn H. L., Hayward, G.N., Nandi, D., Miall, R.C., Aziz, T.Z. and Stein, J.F.(2002). The oscillatory activity in the Parkinsonian subthalamic nucleus investigated using the macro-electrodes for deep brain stimulation. *Clinical Neurophysiology* **113**, 1667-1672.

[19] Liu, X. and Rowe, J., Nandi, D., Hayward, G., Parkin, S., Stein, J. and Aziz, T. (2001). Localisation of the subthalamic nucleus using Radionics Image Fusion and Stereoplan combined with field potential recording. *Stereotact Funct Neurosurg* **76**, 63-73

[20] Kronland-Martinet, R. and Morlet, J. and Grossmann, A. (1987). Analysis of sound patterns through wavelet transforms. *Int J Pattern Recognit Artif Intell*, **1**, 97-126

[21] Mima, T. and Hallett, M. (1999). Electroencephalographic analysis of cortico-muscular coherence: reference effect, **c**onduction and generator *Clin. Neurophysiol.*, **110**, 1892-1899

[22] Mima, T., Steger, J., Gerloff, C. and Hallett, M.(2000). Electroencephalographic measurement of motor cortex control of muscle activity in humans. *Clin. Neurophysiol.*, **111**, 326-337

[23] Perrier, V. and Philipovitch, T. and Basdevant, C. (1995). Wavelet Spectra compared to Fourier Spectra. *J Math Phys*, **36**,1506-1519

[24] Percival, D. (1995). On Estimation of the Wavelet Variance. *Biometrika*, **82**, 619-631

[25] Pezaris, J. and Sahani, M. and Andersen, R. (2000). Spike train coherence in macaque parietal cortex during a memory saccade task. *Neurocomputing*, **32-33**, 953-960

[26] Pope, M.H., Aleksiev, A., Panagiotacopulos, N.D., Lee, J.S., Wilder, D.G., Friesen, K., Stielau, W. and Goel, V.K. (2000). Evaluation of low back muscle surface EMG signals using wavelets. *Clinical Biomechanics*, **15**, 567-573

[27] Priestley, M. (1996). Wavelets and time-dependent spectral analysis. *J Time Seri Anal*, **17**,86-103

[28] Qian, S. (2002). Introduction to Time-Frequency and Wavelet Transforms, *Prentice Hall PTR*

[29] Samar, V. (1999) Wavelet Analysis of Neuroelectric Waveforms. *Brain and Language*, **66**, 1-6

[30] Senhadji, L. and Wendling, F. (2002). Epileptic transient detection: wavelets and time-frequency approaches, *Neurophysiol. Clin.*, **32**, 175-192

[31] Shibata, T. and Shimoyama, I, Ito, T., Abla, D., Iwasa, H., Koseki, K., Yamanouchi, N., Sato, T., and Nakajima, Y. (1998). The synchronization between

brain areas under motor inhibition process in humans estimated by event-related EEG coherence. *Neuroscience Research*, **31**, 265-271

[32] Sinno, D. and Cochran, D. (1992). Invariance of the generalized coherence estimate with respect to reference channel statistics. *IEEE International Conference on Acoustics, Speech, and Signal Processing*, **2**, 505-508

[33] Slobounov, S., Tutwiler, R. Rearick, M. and Ray, W. (2000). Human oscillatory brain activity within gamma band 30-50 Hz induced by visual recognition of non-stable postures. *Cognitive Brain Research*, **9**, 177-192

[34] Tate, A.J., Nicol, A.U., Fischer, H., Segonds-Pichon, A., Feng, J.F., Magnusson, M.S., Kendrick, K.M. (2005). Lateralised local and global encoding of face stimuli by neural networks in the temporal cortex, *Annual Meeting of Neuroscience* (Oral presentation).

[35] Torrence, C. and Compo, G. (1998). A pratical guide to wavelet analysis. *Bullt Amer Meteo Soci* , **79**, 61-78

[36] Torrence, C. and Webster, P. (1999). Interdecadal changes in the ENSO-Monsoon system. *Journal of Climate*, **12**, 2679-2690

[37] Wang, S., Liu, X., Yianni, J., Christopher Miall, R., Aziz, T.Z. and Stein, J.F. (2004). Optimising coherence estimation to assess the functional correlation of tremor-related activity between the subthalamic nucleus and the forearm muscles. *J Neurosci Methods* **136**, 197-205.